Distributed Control of Inverter-Interfaced Microgrids With Bounded Transient Line Currents

Jiajun Duan, *Student Member, IEEE*, Cheng Wang, *Student Member, IEEE*, Hao Xu, *Member, IEEE*, Wenxin Liu, *Senior Member, IEEE*, Jian-Chun Peng, *Senior Member, IEEE*, and Hui Jiang

***Abstract*—Distributed generators (DGs) in a microgrid are tightly coupled through power lines, whose dynamics should not be ignored. If not properly handled, large transient line currents may trigger false protection even under normal operating conditions. Droop-based control adjustments also unnecessarily increase frequency and voltage oscillations. Targeting at these problems, this paper presents a distributed control solution for inverter-interfaced microgrids. The objective of primary control is to realize the desired regulations of bus voltages and frequency as well as suppression of transient line currents. The objective of secondary control is to maintain fair load sharing. At secondary control level, a consensus algorithm is introduced to calculate the references for phase angles of bus voltages based on fair load sharing and dc power flow. At primary control level, a feedback linearization based control algorithm with dynamic control bounds is designed for voltage regulation and transient line current suppression. In addition to a common reference frame, the subsystem controllers only require measurements of local and neighboring subsystems. The effectiveness of the proposed control solution is demonstrated through simulations based on both simplified and detailed models.**

***Index Terms*—Distributed generator (DG), feedback linearization, inverter-interfaced microgrids, transient line current.**

I. Introduction

AN INVERTER-INTERFACED distributed generator (DG) is the basic building block of the rising microgrid paradigm [1]. Various types of DG, such as photovoltaic, wind turbine, and fuel cell, are interfaced to the microgrid through power electronic converters/inverters [2]. The inverter-interfaced DGs are flexible and have fast response speed. Such advantages make DGs easier to operate and control than conventional synchronous generators (SGs) [3]. However, controlling microgrids consisting of such DGs are challenging due to the negligible inertia and intermittent generations, together with severe load changes. If the challenges are not handled properly, the advantages and potentials of the inverter-interfaced microgrid cannot be fully unlocked. Since microgrid is one of the key components for the future smart grid, its performance somehow determines whether the successful deployment of smart grid can be achieved. Thus, operation and control of microgrids have been a hot research area over the last decade.

There are significant differences between traditional large-scale power systems and inverter-interfaced microgrids [4]. Traditional control solutions, which have been proven to be effective for large-scale power systems, cannot be introduced to microgrids without modifications [4]. The first and the easiest type of solutions is to increase the "virtual" inertia of the inverter-interfaced microgrids so that microgrids can behave similar to the traditional power systems [5]. However, these solutions cannot fully unleash the potential of microgrids in terms of flexibility and response speed. The second category of solutions is to model such microgrids as fully decoupled subsystems with impacts of neighboring subsystems formulated as measurable disturbances. At primary control level, droop and inner cascaded loops of proportional–integral (PI) controls are deployed to track the control references regulated by the upper secondary control level. Since microgrids are modeled similar to that of unmanned vehicle systems that have no physical connections among subsystems, many existing solutions in cooperative control [6]–[7], optimal control [8]–[9], and game theory [10]–[11] can be introduced. In the past years, there are many successful developments along this route. These works definitely promote researches on microgrid controls and help bridge the gaps among related societies, especially controls, power systems, and power electronics [5]–[11]. However, there are still many open problems that deserve further investigation.

In general, existing solutions that combine traditional primary control and advanced secondary control have several prob-

Manuscript received October 31, 2016; revised October 26, 2017; accepted December 17, 2017. Date of publication January 18, 2018; date of current version May 2, 2018. Paper no. TII-16-1270. *(Corresponding author: Wenxin Liu.)*

J. Duan, C. Wang, and W. Liu are with the Department of Electrical and Computer Engineering, Lehigh University, Bethlehem, PA 18015 USA (e-mail: jid213@lehigh.edu; chwang925@gmail.com; wliu@lehigh.edu).

H. Xu is with the Department of Electrical and Biomedical Engineering, University of Nevada, Reno, Reno, NV 89557 USA (e-mail: haoxu@unr.edu).

J.-C. Peng is with the College of Mechatronics and Control Engineering, Shenzhen University, Shenzhen 518060, China (e-mail: jcpeng@szu.edu.cn).

H. Jiang is with the Department of Mechatronics and Control Engineering, Shenzhen University, Shenzhen 518060, China (e-mail: huijiang@szu.edu.cn).

Color versions of one or more of the figures in this paper are available online at http://ieeexplore.ieee.org.

Digital Object Identifier 10.1109/TII.2018.2791988

lems. Discussions below summarize these problems in terms of modeling, control objective, and control strategy. First, the line dynamics in microgrids should not be ignored during the control designs [12]. Unlike traditional power systems whose line dynamics are negligible compared to the much slower SG, the line impedances of microgrid are in the same range of the parameters of output filters of DGs [6], [12]. Ignoring the strong physical coupling may cause large transient line current that could trigger false protections. Second, the control objective is usually formulated to manage the capacitor voltages of the *LC/LCL* output filters instead of terminal voltage, which affects loads directly. Since terminal bus voltage is not directly under control, small voltage control deviation is unavoidable. Third, such control strategy unnecessarily excites frequency oscillations due to the deployment of frequency droop control [13]. Unlike SG, the electrical frequency of inverter-interfaced DG is not linked to a mechanical speed that may oscillate during changes of operating conditions. Adjusting frequency references is possible to simplify control design, but it also degrades frequency response.

To solve the above challenging problems, related aspects of control engineering need to be revisited. If line dynamics are considered during the control design, the microgrid system can no longer be treated as an integration of fully decoupled subsystems. Since traditional primary control is decentralized (myopic) and upper control levels target at (economical) coordination and correction, conventional hieratical control schemes have no control over the transient line currents. To regulate the transient line currents, communications among the DG controllers and/or between the DGs and the central controller become necessary. The introduction of communications makes primary control no longer decentralized (communication free). Actually, centralized or intersubsystem communications have already been used explicitly in secondary control and/or implicitly in primary control, such as during reference frame synchronization and system frequency evaluation [12]. It has been demonstrated that moderate amount of intersubsystem communications can significantly improve the control performance by increasing global situational awareness [14]. Nowadays, the speed and reliability of communication systems have been significantly improved. Preference should not be given to the decentralized control design. Control performance and required amount of communications should be better balanced. The reliability and security aspects of the communication system can be addressed in the future.

In this paper, a distributed control solution is presented for microgrids that consist of multiple inverter-interfaced DGs with *L* filters. The objective of primary control is to realize good regulations of system frequency and load bus voltages, whereas the objective of secondary control is to achieve fair load sharing. Moreover, at the upper control level, a distributed consensus-based load sharing algorithm is introduced to obtain the desired power generation references, which are subsequently used to decide the phase angle references of bus voltages through dc power flow. At primary control level, the phase angles are used to decide the *dq* components of bus voltage references. In order to counteract the uncertainty and impreciseness, droop equations are applied to adjust the secondary phase angle references among reference updating intervals. The mode of bus voltage regulation is overridden by the mode of line current suppression

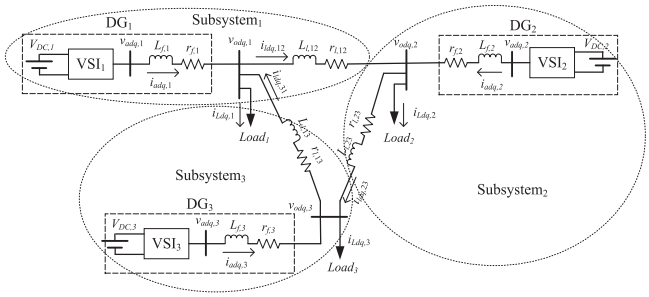

Fig. 1. Schematic diagram of an inverter interfaced microgrid.

whenever line currents approach the predetermined bounds. In this way, the interests of customers (frequency and voltage) and utility (efficiency and reliability) can be well coordinated. Except for evaluating the simplified model based algorithm, the proposed solution is also tested through a detailed model to demonstrate the robustness of the feedback linearization based control algorithm under model impreciseness. The contributions of this paper are summarized as follows.

1) Both secondary and primary control problems of ac microgrids are reformulated. The benefits of utilities and customers are better coordinated.
2) A distributed secondary controller is designed for DG coordination and a distributed primary controller is developed to coordinate bus voltage (first priority objective) and transient line current (second priority objective).
3) The proposed distributed solution can increase the flexibility of the system compared to the centralized control. The simple control design based on *L* filter can be extended to other applications (e.g., *LC* filter), which can reduce the complexity and improve the applicability of control implementation.
4) Except for protecting the sensitive load and avoiding the false triggering of protection system, the proposed control method can greatly increase the system reliability when the microgrid is approaching its upper limit of capacity. In addition, the proposed control scheme also considers the situation under system fault.

The rest of this paper is organized as follows. Section II introduces the formulation of the microgrids control problem. Section III presents the designs of the primary and secondary control. Section IV provides the simulation results with both simplified and detailed microgrids models. Section V provides the concluding remarks and discusses the future work.

II. Formulation of the Microgrid Control Problem

Without loss of generality, Fig. 1 shows the schematic diagram of a microgrid consisted of three DGs with *L* filters. For each DG, a voltage source inverter is connected to a dc source that stands for the direct or intermediate output of a distributed renewable or traditional energy source. *L* filter is connected between the inverter and the bus, and then connected to the rest of microgrids. The filters are important for current harmonic filtering and voltage stabilization [15]. Each DG may or may not have a load directly connected to its output filter/bus. Multiple

DGs and loads join together through power lines to form an integral inverter-interfaced microgrid.

Due to the fast response of power converters, the RLC components of output filter and power lines are actually dominating system's transient response. Thus, their dynamics should be included into the average control model, which is more suitable for control design and implementation than a switch-level model. For convenience, the model used in control design is summarized as follows.

The state equations governing the *L*-filter dynamics for *i*th inverter are presented as

$$\dot{i}_{ad,i} = -\frac{1}{L_{f,i}}(r_{f,i}i_{ad,i} + v_{od,i}) + \omega_n i_{aq,i} + \frac{1}{L_{f,i}}v_{ad,i} \quad (1)$$

$$\dot{i}_{aq,i} = -\frac{1}{L_{f,i}}(r_{f,i}i_{aq,i} + v_{oq,i}) - \omega_n i_{ad,i} + \frac{1}{L_{f,i}}v_{aq,i} \quad (2)$$

where $L_{f,i}$ is the inductance of *L* filter, $r_{f,i}$ is the parasitic resistances of the inductor, ω_n is the nominal electrical angular velocity, $v_{od,i}$ and v_{oqi} are *dq* components of the load bus voltage of the *i*th subsystem ($v_{\mathrm{o,i}}$), and $v_{ad,i}$ and $v_{aq,i}$ are the *dq* components of the output voltage of *i*th DG ($v_{\mathrm{a,i}}$).

Assuming that a power line is connecting buses *i* and *j*, and its dynamics can be represented as

$$\dot{i}_{ld,ij} = \frac{1}{L_{l,ij}}(-r_{l,ij}i_{ld,ij} + v_{od,i} - v_{od,j}) + \omega_n i_{lq,ij} \quad (3)$$

$$\dot{i}_{lq,ij} = \frac{1}{L_{l,ij}}(-r_{l,ij}i_{lq,ij} + v_{oq,i} - v_{oq,j}) - \omega_n i_{ld,ij} \quad (4)$$

where $r_{l,ij}$ represents the resistance of the power line linking buses *i* and *j*, $L_{l,ij}$ is the lumped inductance of the power line, and $i_{ld,ij}$ and $i_{lq,ij}$ are the *dq* components of line current $(i_{l,ij})$.

In order to roughly predict the load perturbation effects and obtain the representation of bus voltage for accurate voltage control [12], the virtual resistance method can be used as

$$v_{od,i} = r_n(i_{ad,i} - i_{ld,i} - i_{Ld,i}) \quad (5)$$

$$v_{oq,i} = r_n(i_{aq,i} - i_{lq,i} - i_{Lq,i}) \quad (6)$$

where $i_{ld,i} = \sum_1^{n_i} i_{ld,ij}$ and $i_{lq,i} = \sum_1^{n_i} i_{lq,ij}$ are the *dq* components of the overall line current leaving bus *i* $(i_{ldq,i})$ with n_i being the number of buses connected to bus *i*, $i_{Ld,i}$ and $i_{\mathrm{Lq,i}}$ are the *dq* components of load current at bus *i* $(i_{L,i})$, and r_n is a large virtual resistance, whose value should be large enough to minimize any impact on system dynamics.

Equations (1)–(6) represent the formulation of one subsystem, and a completed microgrid model is composed of multiple such subsystem models. Such model can represent a general class of microgrids whose loads are directly connected to the DG buses instead of intermediate buses. It should be noted that the abovementioned linear equations will result in a nonlinear control problem if the control objective is to regulate quantities that are represented as nonlinear functions of system states, e.g., output voltage $(V_{o,i})$ and active power.

Generally, each subsystem has its own *dq* reference frame. In order to integrate multiple subsystem models together, a common reference frame is needed. There are two methods to determine the common reference frame, which is a signal that can be represented as $\cos(\omega(t)^*t + \theta)$. The first method is to make dynamic measurements at one of the DGs and use it as the system-wide reference. The other method is to use a common reference signal generated by an accurate clock or function generator. Both methods require communications between the source reference signals and the recipients either in a centralized way or in a distributed way.

Since the frequency of the reference DG changes along with time, the first method will constantly create a large disturbance to phase-locked loop (PLL). Thus, dynamics of PLL are usually considered for the first method, which complicates the control design. In contrast, a reference signal of the second method has a constant frequency, and frequency oscillations can be minimized through constant frequency reference setting (60 Hz). Since each DG is utilizing the same reference information, PLL is not required for the second method, which decreases the difficulties with control design and implementation. The communication requirement of the second method can be further reduced if each subsystem has an accurate clock, which can be obtained with a GPS receiver. In that case, only periodical correction or distributed clock synchronization is needed to maintain clock accuracy and synchronization.

In a power system, there are four performance indices, which are active power generation (*P*), reactive power generation (*Q*), bus voltage (*V*), and system frequency (*f*). Among the four performance indices, *V* and *f* are more important for loads, whereas utilities care more about *P* and *Q*. Of course, all four of them are important for a power system to operate effectively. However, these four quantities are coupled in a complicated way in the power systems. Due to the complex relationship and conflicts among them, it is very difficult and even impossible to realize perfect control of all quantities simultaneously. During control design process, the four quantities should be carefully selected and prioritized based on system characteristics and operation requirements.

III. Control Design For Inverter-Interfaced Microgrids

Currently, there are two popular control modes for microgrids, i.e., *V–f* control and *P–Q* control [16]. These two control modes target at different concerns or operating conditions. For *V–f* control, the control objective is to maintain the constant RMS bus voltages and system frequency. For *P–Q* control, the control objective is to track the *P* and *Q* references that are calculated based on system-wide efficiency and static stability considerations. To counteract the impacts of an unavoidable load change and inaccuracy during reference setting, adjustments based on predefined droop characteristics are usually deployed. The introduction of droop control may cause voltage and frequency deviations that have to request periodic correction by upper level controller [4], [13].

There are significant differences between inverter-interfaced microgrids and SG-based large-scale power systems. For an SG, the physical rotor speed adjusts to charge or discharge its mechanical potential energy during supply–demand imbalance. The rotor speed reflects an electrical frequency based on the

construction of SG. Since f is linked to P, it is necessary and reasonable to deploy P–f droop control in traditional power systems. However, there is no such physical P–f coupling in the inverter-interfaced microgrids due to the decoupling of dc source and ac generation. Since the frequency of inverter-interfaced DG can be easily regulated around 60 Hz, using droop control to adjust frequency during load change unnecessarily increases frequency oscillations. If each subsystem adjusts its frequency reference separately, multiple frequencies will appear in the system during transient states. It not only disturbs the convergence of PLL, but also causes difficulty for frequency evaluation.

It is a common sense that energy efficiency (P and Q optimization) becomes secondary compared to stability (V and f regulation). In the proposed control design, the primary control objective is load bus voltage (V) regulations, and the secondary control objective is fair load sharing (P). f reference is set to be a constant, and Q is not directly regulated. For the reference set of bus voltage, the RMS value is fixed and only phase angle is adjusted. In this way, the voltage can be well stabilized as the other critical quantity, i.e., f. The adjustment of the voltage phase angle considers both fair load sharing and complexity of uncertain operating conditions. This control strategy full considers the priority of control objectives while trying to keep flexibility and efficiency. In order to guarantee fast and smooth tracking of the control references and avoid a surge of line current, a novel control algorithm needs to be designed.

Based on above-mentioned introduction, one can tell that the solution should consist of two control levels for larger time-scale and real-time coordination of subsystems, respectively. The upper level secondary control is in charge of control reference setting, whereas the lower level primary control is responsible for control reference adjustment and tracking. Details of the proposed control solution are presented in the following sections.

A. Secondary Control Design

The objective of secondary control is to find the phase angles references (δ^*) of the bus voltages $(V_o\angle\delta)$ based on operational constraints in a two-step procedure. First, generation references of the DGs (P_G^*) are decided based on a consensus-based distributed algorithm presented in [17]. Second, the generation references (P_G^*) together with desired bus voltages (V_o^*) are used to decide the bus phase angles (δ^*). These two steps are separately introduced as follows.

As introduced in [17], the objective of fair load sharing is to find a common utilization level, which is decided according to the overall demand and maximum generation. The overall demand includes both demands of the loads and the estimated system-wide active power loss. The overall maximum generation is decided by the total predicted intermittent generations and the physical generation limit of nonintermittent generations. Since a consensus algorithm can find the global average of distributed signals, it can be used to explore the average demand and average maximum generation through distributed communications. Once the DGs obtain these two quantities, they can calculate local utilization levels, which is same for all of DGs. By synchronizing the utilization level, fair load sharing can be realized and the impact of inaccurate generation prediction can be minimized.

After the generation references (P_G^*) are obtained, the corresponding voltage phase angles references (δ^*) have to be determined through power flow to realize the desired load sharing. To do that, the DG with the largest capacity is selected as the slack bus with flexible generations. Both ac and dc power flow can be realized in a distributed manner such as in [18]. Since slight inaccuracy is not as important as response speed, distributed dc power flow is a better choice for this purpose. In addition, dc power flow can be achieved within predetermined steps (time), which helps in improving the reliability and certainty of solutions. Thus, it enables more timely control reference updating for large-scale microgrids. It should be noted that the outcome of power flow study is defined as δ_i', which is not same as the final reference $\delta_i{}^*$.

B. Primary Control Design

1) Control Reference Adjustment: Because the inaccuracy during control reference setting and operating condition changes between reference updating intervals is unavoidable, there should be a way to adjust the control reference continuously or periodically in a more frequent manner (compared to the frequency of updating δ_i'). Therefore, a simple phase angle droop equation of (7) is used to adjust the phase angle based on the deviation of actual generation $(P_{G,i})$ from the expected generation (P_{Gi}^*) [19]

$$\delta_i^* = \delta_i' - K_{\delta i}(P_{G,i} - P_{G,i}^*) \tag{7}$$

where $K_{\delta i}$ is the droop coefficient determined based on the steady-state performance criteria [4].

Once the voltage phase angles are decided, the dq components of the bus voltage references $v_{od,i}^*$ and $v_{oq,i}^*$ can be calculated according to the following equation:

$$\begin{cases} v_{od,i}^* = V_{o,i}^* \cos(\delta_i^*) \\ v_{oq,i}^* = V_{o,i}^* \sin(\delta_i^*) \end{cases} \tag{8}$$

where $V_{o,i}^*$ is the RMS voltage reference at bus i.

By tracking the control references ($v_{od,i}^*$, $v_{oq,i}^*$, and $f^* = 60$ Hz), the primary control objectives (V and f regulation) can be well achieved and the secondary control objective (P_{G}^*) can also be approached.

2) Control Reference Tracking: The designed algorithm has two modes of control with respect to bus voltage regulation and transient line current suppression, respectively. Details are given as follows.

a) Bus voltage regulation: To better regulate the bus voltages, a feedback linearization based control algorithm is designed.

According to (9), the tracking errors of bus voltage can be defined as

$$\begin{cases} e_{od,i} = v_{od,i} - v_{od,i}^* \\ e_{oq,i} = v_{oq,i} - v_{oq,i}^* \end{cases}. \tag{9}$$

Since $v_{od,i}^*$ and $v_{oq,i}^*$ are updated periodically, they can be treated as constants between control updating intervals. Based

on (5) and (6), the dynamics of voltage tracking errors can be reformulated as

$$\begin{cases} \dot{e}_{od,i} = f(e_{od,i}) + B_{od,i} v_{ad,i} \\ \dot{e}_{oq,i} = f(e_{oq,i}) + B_{oq,i} v_{aq,i} \end{cases} \tag{10}$$

where

$$f(e_{od,i}) = r_n \begin{Bmatrix} -\frac{1}{L_{f,i}}(r_{f,i} i_{ad,i} + v_{od,i}) + \omega_n i_{aq,i} - \omega_n i_{lq,i} \\ -\frac{1}{L_{l,ij}}(-r_{l,ij} i_{ld,i} + v_{od,i} - v_{od,j}) - \dot{i}_{Ld,i} \end{Bmatrix},$$

$$B_{od,i} = B_{oq,i} = \frac{r_n}{L_{f,i}},$$

and

$$f(e_{oq,i}) = r_n \begin{Bmatrix} -\frac{1}{L_{f,i}}(r_{f,i} i_{aq,i} + v_{oq,i}) - \omega_n i_{ad,i} + \omega_n i_{ld,i} \\ -\frac{1}{L_{l,ij}}(-r_{l,ij} i_{lq,i} + v_{oq,i} - v_{oq,j}) - \dot{i}_{Lq,i} \end{Bmatrix}.$$

According to the theory of feedback linearization [20], the control signals can be designed as

$$\begin{bmatrix} v_{ad,i} \\ v_{aq,i} \end{bmatrix} = \begin{bmatrix} \frac{1}{B_{od,i}} \left[-f\left(e_{od,i}\right) - K_{od,i} e_{od,i} \right] \\ \frac{1}{B_{oq,i}} \left[-f\left(e_{oq,i}\right) - K_{oq,i} e_{oq,i} \right] \end{bmatrix} \tag{11}$$

where $K_{od,i}$ and $K_{oq,i}$ are positive design parameters.

Substituting designed control (11) into (10), the tracking errors can be represented as

$$\begin{cases} \dot{e}_{od,i} = -K_{od,i} e_{od,i} \\ \dot{e}_{oq,i} = -K_{oq,i} e_{oq,i} \end{cases}. \tag{12}$$

Since $K_{od,i}$ and $K_{oq,i}$ are positive design parameters, it is easy to demonstrate that tracking errors will converge to zeros asymptotically [21].

Above control algorithm is very similar to other feedback linearization based primary control algorithms that are developed for microgrids control [22]. The only difference is with the control formulation (control model and control objectives). It is important to note that the algorithm is distributed in the sense that signals for subsystem control computation are all locally measurable.

b) Transient line current suppression: Above control algorithm and most other primary control algorithms for microgrids have no control over transient line currents. Neither can any upper level secondary control algorithms, which are only able to address steady-state constraints of line currents periodically at a larger time scale. The unexpected transient line current surge makes tuning of protection system difficult and may cause huge losses due to false fault protections. For a well-designed microgrid, the line currents should always stay within their loadability limits during the normal operating conditions [23]. Thus the easiest solution for transient line current suppression is to restrict the line currents within reasonable constant bounds.

Based on current values of $i_{ld,ij}$ and $i_{lq,ij}$, their derivatives formulated as (3) and (4), and the selected time step (T_s), the next-step values of $i_{ld,ij}$ and $i_{lq,ij}$ can be estimated. Based on the estimated values, the line current constraint $i_{l,ij}^2 = i_{ld,ij}^2 + i_{lq,ij}^2 \le \bar{i}_{ij}^2$ is evaluated. Should the constraint be violated, the following control signals limitation is proactively activated.

A straightforward solution is to make the derivative of $i_{l,ij}^2$ negative. In this way, the combined range of the control inputs, i.e., $v_{ad,i}$ and $v_{aq,i}$, can be determined. The range is used to compare with the control signals calculated for voltage regulation (11). However, two vectors cannot be directly compared before certain norm function is introduced. Even after that, control adjustment based on norm comparison will still be a problem.

In order to perfectly solve this problem, a complicated control algorithm has to be designed due to the strong coupling of subsystems. To reduce the complexity, a simple heuristic solution is presented below. The control objective is not to limit $i_{l,ij}^2$, but to decrease the dq components $i_{ld,ij}^2$ and $i_{lq,ij}^2$ simultaneously, while the line current constraint is not satisfied. It should be noted that the method is a sufficient condition rather than a necessary and sufficient condition. Deriving a necessary and sufficient condition is similar to find the perfect solution mentioned above, which is difficult for design and implementation. As can be seen later, the simplified method can generate the decouple bounds for control signals. Thus, subsequent control implementation becomes easy.

Based on (1)–(4), in order to lower/maintain $i_{ld,ij}^2$ and $i_{lq,ij}^2$ at the same time, the following two conditions need to be satisfied:

$$\begin{cases} d\left(i_{ld,ij}^2\right)/dt = 2 i_{ld,ij} \dot{i}_{ld,ij} = f_{dl,ij}(\bullet) \\ \qquad\qquad + g_{dl,ij}(\bullet) v_{ad,i} \le -|b_d| \\ d\left(i_{lq,ij}^2\right)/dt = 2 i_{lq,ij} \dot{i}_{lq,ij} = f_{ql,ij}(\bullet) \\ \qquad\qquad + g_{ql,ij}(\bullet) v_{aq,i} \le -|b_q| \end{cases} \tag{13}$$

where

$$f_{dl,ij}(\bullet) = -\frac{2 r_{l,ij}}{L_{l,ij}} i_{ld,ij}^2 - \frac{2 i_{ld,ij}}{L_{li,j}} \times \left(r_{f,i} i_{ad,i} - \omega_n L_{f,i} i_{aq,i} + L_{f,i} \dot{i}_{ad,i}\right) - \frac{2 i_{ld,ij}}{L_{l,ij}} v_{od,j},$$

$$f_{ql,ij}(\bullet) = -\frac{2 r_{l,ij}}{L_{l,ij}} i_{lq,ij}^2 - \frac{2 i_{lq,ij}}{L_{l,ij}} \times \left(r_{f,i} i_{aq,i} + \omega_n L_{f,i} i_{ad,i} + L_{f,i} \dot{i}_{aq,i}\right) - \frac{2 i_{lq,ij}}{L_{l,ij}} v_{oq,j},$$

$g_{dl,ij}(\bullet) = \frac{2 i_{lq,ij}}{L_{l,ij}}$, $g_{ql,ij}(\bullet) = \frac{2 i_{ld,ij}}{L_{l,ij}}$, and $|b_d|$, $|b_q|$ are positive constants, and take 1.7 and 1.5, respectively.

Thus, the following two bounds on control signals need to be applied simultaneously to decrease transient line current

$$\begin{cases} v_{ad,i} \le -g_{dl,ij}^{-1}(\bullet) \left[|b_d| + f_{dl,ij}(\bullet)\right] \equiv \bar{v}_{ad,i} \\ v_{aq,i} \le -g_{ql,ij}^{-1}(\bullet) \left[|b_q| + f_{ql,ij}(\bullet)\right] \equiv \bar{v}_{aq,i} \end{cases}. \tag{14}$$

Based on the definitions of the $g_{dql,ij}$ and $f_{dql,ij}$, one can see that measurements of the local and neighboring subsystems are required to calculate the bounds of local control signals. This effort is necessary to restrict the transient line current. Once overline current is predicted, the bounds $\bar{v}_{ad,i}$ and $\bar{v}_{ad,i}$ of (14) are used to clamp the control signals calculated according to (11). In this way, transient line current can be restricted and this process does not have an excessive impact on voltage control performance.

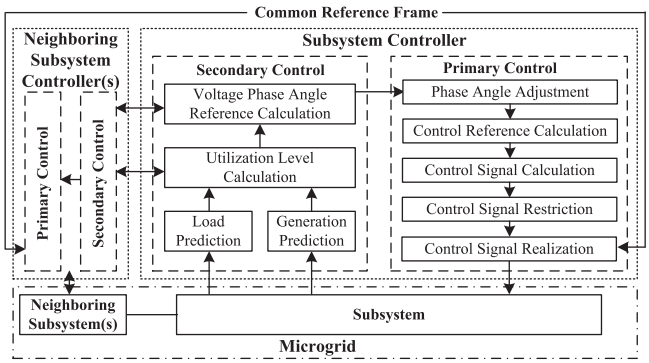

Fig. 2. Flowchart diagram of the proposed microgrid control scheme.

TABLE I
PARAMETERS OF MICROGRID

Parameter	Value	Description
r_{f1}, r_{f2}, r_{f3}	0.50, 0.51, 0.52 Ω	Filter resistance
L_{f1}, L_{f2}, L_{f3}	4.21, 4.20, 4.215 mH	Filter inductance
$r_{line12}, r_{line23}, r_{line31}$	0.151, 0.152, 0.154 Ω	Line resistance
$L_{line12}, L_{line23}, L_{line31}$	0.42, 0.41, 0.414 mH	Line inductance
R_n	1000 Ω	Virtual resistance
K_p	1/1000 rad/W	Droop control gain
K_{od}	3.2	Control gain
K_{oq}	3.2	Control gain
ω_n	377 rad/s	Nominal angular velocity
T_s	10^{-4} s	Time step

C. Control Implementation

Implementation of the overall control solution is illustrated in Fig. 2. To initialize the consensus-based load sharing algorithm, load and maximum generation over the projected period are estimated. Finding the synchronized utilization level requires communications between subsystem controllers. After the convergence of the utilization level, generation references of all subsystems can be calculated. Based on generation references, bus voltage settings, and power line parameters, distributed dc power flow is introduced to calculate the phase angle references of the bus voltages. The distributed operation also requires direct interactions of subsystem controllers. The phase angle references are adjusted in real time based on a simple δ–P_{G} droop equation. The adjusted phase angle references together with RMS values of bus voltages are used to generate the *dq* components of the bus voltage references.

During the normal operating conditions, the control objective is to make the bus voltages track the corresponding references. Whenever a line current bound violation is predicted, control signals are bounded to ensure an immediate decrease in line current. Then, *dq* components of the control signals are converted to *abc* components through *dq*–*abc* transformation. Based on a predefined common reference frame rotating at a constant frequency (60 Hz), the common phase angle reference can be found by the integration of frequency (ωt). Due to the fast response of inverter-interfaced DGs, the frequency reference track can be finished instantly. Therefore, each subsystem controller takes the general information of phase angle from the common reference frame to perform the *dq*–*abc* or *abc*–*dq* transformation. Finally, pulse width modulation (PWM) signals are generated from the final control signals to realize the desired control performance.

To lower the computational complexity of the control algorithm, the next-step line current prediction can be replaced by simply comparing the line current against a constant bound $\bar{i}_{ij}$. Once the line current is larger than the bound, control signals will be bounded according to (14). It is true that this way of implementation will cause certain inaccuracy. However, the inaccuracy can be neglected due to several reasons. First, line current will not increase abruptly within a small time step T_{s} due to the inductance in the system. Second, the degradation of control performance is smaller than that due to an imprecise model and uncertain operating condition. Third, the line current bound is usually set to a value slightly smaller than the physical hard limit. Thus, the simplified method is implemented during the simulation evaluation.

IV. SIMULATION RESULTS

In order to evaluate the performance of the proposed control solution, simulations with both the mathematical model and detailed model are carried out using MATLAB/Simulink. Parameters of a three-DG microgrid model and control gains are provided in Table I, which is modified based on [12]. The proposed solution is also compared to the conventional PI-based primary control algorithm [12]. In order to avoid the divergence and make the comparison illustrative, the PI-based primary control method is combined with the secondary control method, as proposed in this paper.

A. Case I: Simulation With Mathematical Microgrid Model

During the primary control algorithm test, maximum generations are held fixed and a step change of constant load is simulated. Implementation details and performance of the secondary control algorithms can be found in the referred paper [17]. In this case, the secondary control algorithm is only activated once at the instant of time of load change.

The simulation starts from the steady state and a step load change is simulated at 0.1s. The maximum generations of three generator references are 1.30, 1.05, 0.90 per unit (p.u.) respectively, and held constant during the 3-s simulation. Three active power loads before and after the load change are 0.70, 0.60, and 0.48 p.u. and 0.58, 0.80, and 0.60 p.u., respectively. The initial generation references are 0.712, 0.575, and 0.492 p.u., which is obtained based on the estimated maximum generations. Based on dc power flow and the RMS voltage settings of 1.0, 1.0, and 1.0 p.u., the phase angles reference before load change are 0, 0.04, and 0.01 rad. Under this simulation setting, the generation reference and phase angels reference after load change are 0.792, 0.636, and 0.548 p.u. and 0.042, –0.028, and 0.035 rad, respectively. After transients damped out under previous control, the actual generations with and without bound are 0.793, 0.640, and 0.541 p.u. and 0.791, 0.660, and 0.530 p.u., respectively. The actual phase angels of both controllers (with

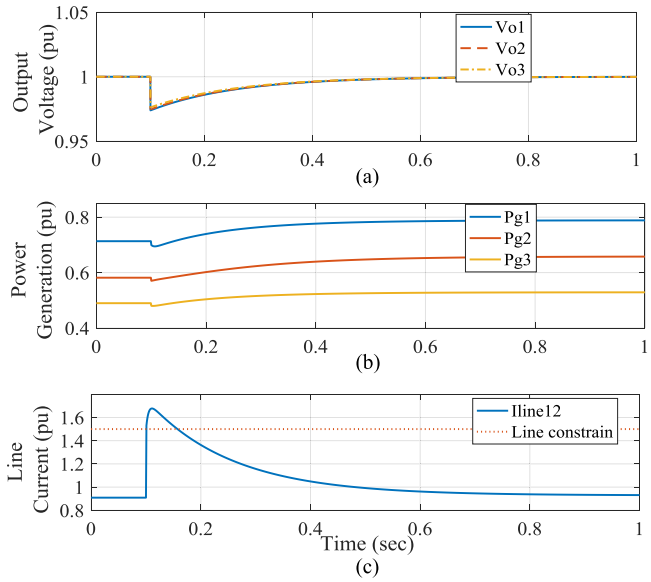

Fig. 3. Simulation results of control scheme without considering line current constraint. (a) Load bus voltages $(v_{o,i})$. (b) Power generation $(P_{G,i})$. (c) Line current $(i_{l,i})$.

and without bound) succeed in converging to the desired phase angle references after the load change (0.042, –0.028, and 0.035 rad).

At first, the line current constraint is not applied. The corresponding responses of load bus voltages and power generation are shown in Fig. 3(a) and (b), respectively. As can be seen, both bus voltage and power generation are able to track their references well before and after the load change. In Fig. 3(c), a large line current surge (at line_{12}) can be observed at the beginning of load change. It is because current control only targets at voltage references tracking. Thus, in order to suppress the peak transient current, 1.5 p.u. can be selected as the line current bound for algorithm evaluation.

To maintain the transient line current i_{line12} within 1.5 p.u., the corresponding control bound is applied on $v_{adq,1}$, which is in charge of the current limitation of this power line. The responses of bus voltage, power generation, line current, and control signals are shown in the four plots of Fig. 4, respectively. As can be noticed, both bus voltages and power generations succeed in tracking their corresponding references. Besides, the surge current on the power line gets significantly suppressed within 1.5 p.u. As can be seen in the zoomed-in subplot of Fig. 4(c), the line current of i_{line12} touches the bound a few (about 20) times during the initial few time steps of load change. The period is so short that it cannot be noticed in the initial plot. Although the transient bus voltage has a larger drop comparing with the previous one, the overall performance is still within the acceptable range, e.g., 0.95–1.05 p.u. [19]. By comparing Fig. 4(b) and Fig. 3(b), one can see that generations converge in a different way under the line current limitation. It seems that oscillations of generation are smaller due to the suppression of unnecessary current surges. The control signal $v_{ad,1}$ is subjected to the corresponding control bound $\bar{v}_{ad,1}$, and the related responses (dynamic bound, without bound, and with bound) are plotted in

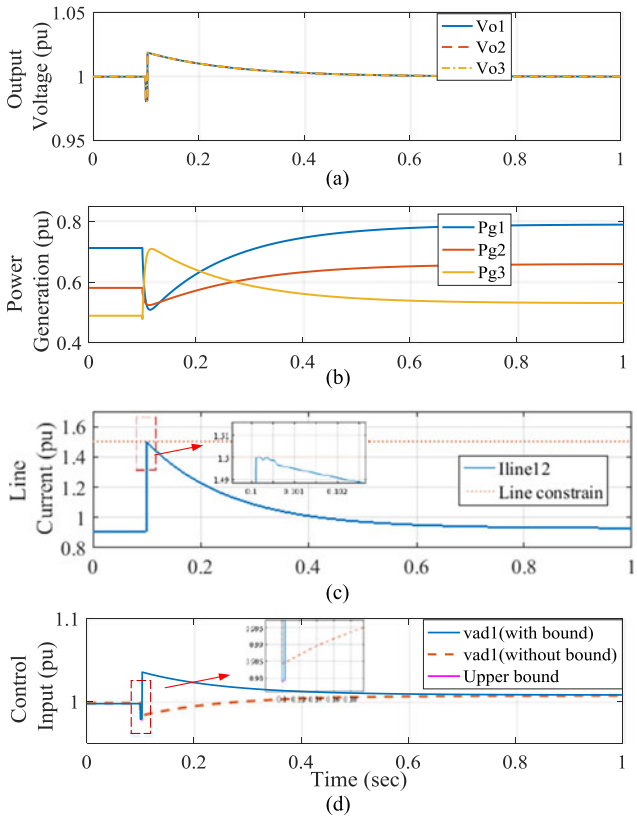

Fig. 4. Simulation results of the proposed control scheme with considering line current constraint: (a) load bus voltages $(v_{o,i})$, (b) power generation $(P_{G,i})$, (c) line current $(i_{l,i})$, and (d) control signals.

Fig. 4(d). It can be seen that the control bounds are triggered only about 20 times, which matches the above observation with line current (i_{line12}). In addition to simplified microgrid model, the proposed control solution is also tested with a detailed microgrid model, as shown in Section IV-B.

B. Case II: Simulation With Average Microgrid Model

The average model is simulated using Simscape Power System toolbox of Simulink. In the simulation, the voltage controlled sources are used in simulation of the DGs. The parameter settings are the same as the mathematical model expects for the constant power loads. In order to better evaluate the performance of the proposed control solution, it is compared to a widely used conventional PI-based control scheme with the proposed secondary control [12]. The parameter settings of the PI-based primary controller can be found in [12]. The total simulation time is 1s, and a load change occurs at 0.1s. The objective of the second case is the same as the first one, which is to maintain the transient line current within 1.5 p.u.

The responses of system frequency, line current i_{line12}, and control input signals are shown in Fig. 5. Because control objectives of the conventional controller are to track the nominal frequency and voltage, its overall performance is quite limited. In addition to large frequency oscillations, significant transient current can be observed. Even though the control parameters can be better tuned, the tuning process is difficult, especially

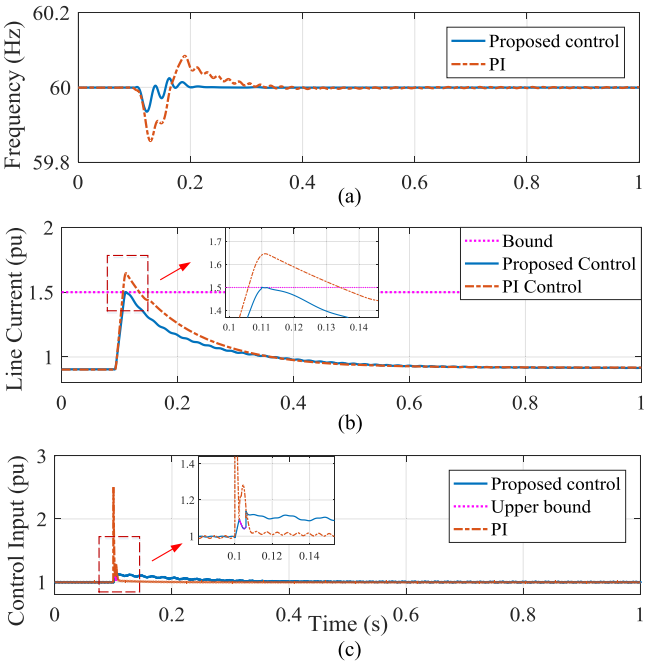

Fig. 5. Simulation results on the average model. (a) System frequency (f). (b) Line current $(i_{l,i})$. (c) Control signal $(v_{ad,i})$.

under a wide range of operating conditions. As can be observed, the proposed controller can not only achieve the desired tracking performance, but can also limit the line current within a predefined range (i.e., 1.5 p.u.). It should be noted that although the inverters have fixed frequency reference, slight oscillations can still be observed in Fig. 5(b). But it is obviously better than that of a traditional solution. The oscillations mainly come from the adjustments of voltage phase angles during a load change. Again, one can see that the control bound is triggered only at the first few steps during peak oscillations. The application of control bounds does change the form of control signal afterward. It should be noted that there are small overshoots beyond the predefined current limit. This is because of two reasons. First, the simplified implementation method discussed in the last section unavoidably introduces small inaccuracies. Second, there are unmolded dynamics in the detailed model such as system inertia, which results in an inaccuracy to the bound calculation. However, the overall performance is still satisfactory. By using a smaller bound or increasing the value of $|b_{\mathrm{d}}|$ and $|b_{\mathrm{q}}|$ in (13), the impact of small overshoots can be mitigated.

The voltage responses of two controllers are shown in Fig. 6. It should be noted that due to the switch between voltage control mode and current control mode, the voltage regulation performance of the proposed controller is little bit decreased. However, the overall performance is still satisfactory and the operating range of the original system has been greatly expanded.

C. Case III: Simulation With Switching-Level Microgrid Model

In this case, more details are considered in the switching-level model, such as PWM generator, two-level inverter, and *dq–abc* transformation. In order to further reduce the total harmonic

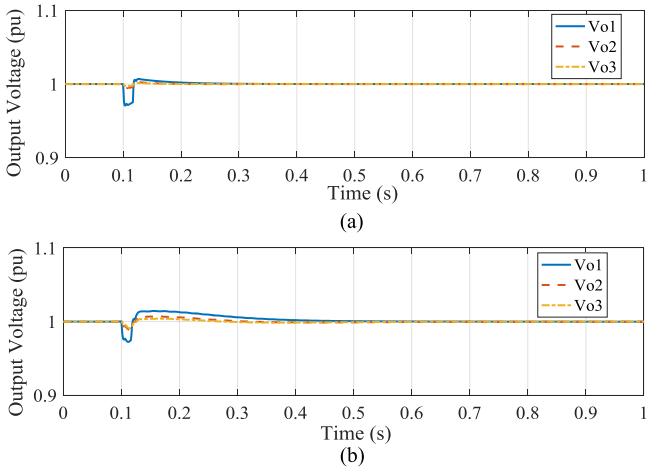

Fig. 6. Bus voltage responses on the average model. (a) PI controller. (b) Proposed controller.

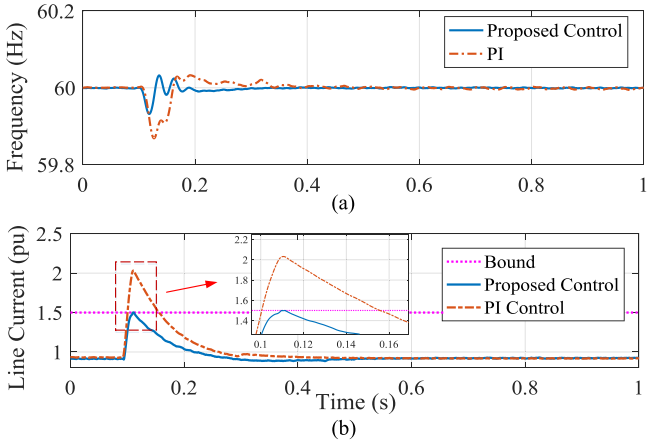

Fig. 7. Simulation results on switching-level model. (a) System frequency (f). (b) Line current $(i_{l,i})$.

distortion (THD) of the system, *LC* filters are utilized in the simulation. Since the capacitor of the *LC* filter can be treated as one part of the load, there is no need to modify the control algorithm. For some specific application, the decision on installation and size of the capacitor can be made based on an actual loading condition and the requirement on THD. In the simulation, *LC* filters with 20 μF capacitance are used. The control objectives remain to regulate the bus voltage while keeping the transient line current within 1.5 p.u. The rest of the system setting is also the same as in the previous cases. The simulation results including system frequency and line current are shown in Fig. 7, and the voltage responses are presented in Fig. 8, respectively. As can be seen, the simulation results on the detail switching-level model match with those on the simplified model. The proposed controller is able to achieve the designed targets on voltage and current. In addition, due to the usage of *LC* filter, only a little bit harmonic appears in the detailed simulation. It also reflects the main advantages of the proposed control algorithm in terms of simplicity, generality, and flexibility.

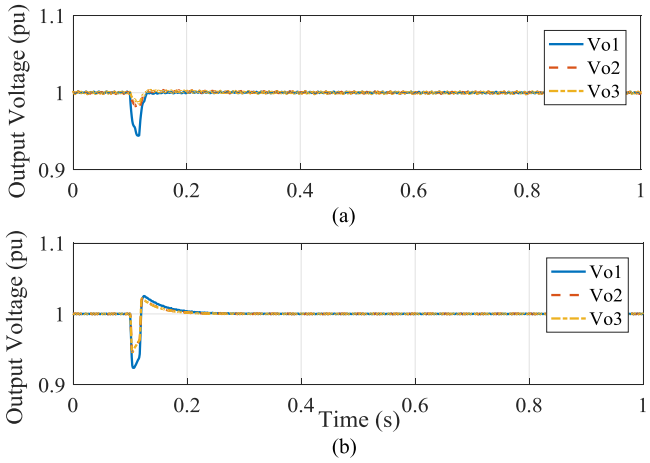

Fig. 8. Bus voltage responses on switching-level model. (a) PI controller. (b) Proposed controller.

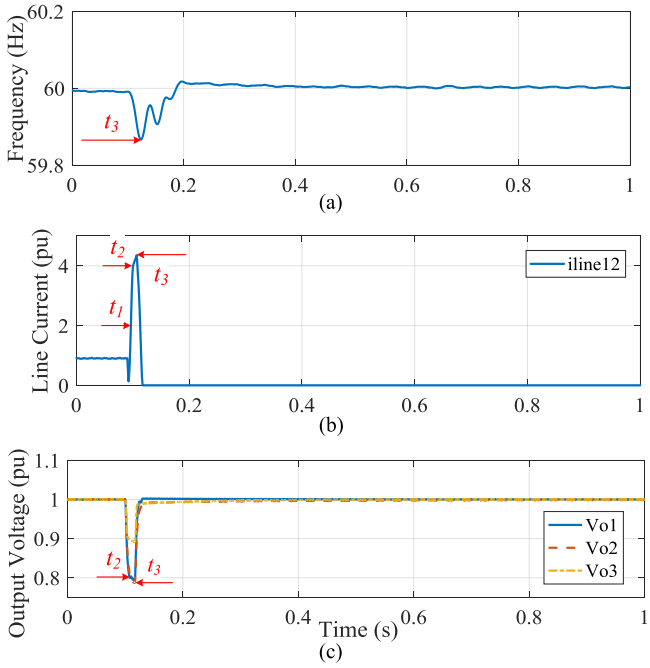

Fig. 9. Simulation results on a switching-level model during system fault. (a) System frequency (f). (b) Line current $(i_{l,i})$. (c) Bus voltage $(v_{o,i})$.

D. Case IV: Simulation Under System Fault

In this section, the proposed control algorithm is tested under the extreme system condition, i.e., system fault. In order to keep the system stable, as long as the voltage deviation is more than ± 0.2 p.u. of the nominal value, the controller will be fixed in the voltage control mode. At the same time, the circuit breaker is supposed to be triggered to clear the fault line whenever the current is beyond 2.0 p.u. The simulation results are presented in Fig. 9. There are several time-critical nodes that are worth mentioning. At time 0.1 s, a three-phase short circuit occurs between buses #1 and #2. Before time t_2, the controller has been switched to the current control mode and try to suppress the line current. At time t_2, the controller is fixed in the voltage control mode once the voltage deviation is beyond 0.2 p.u. Circuit breakers are triggered at the point when line current reaches 2.0 p.u. at time t_1. After one cycle, at time t_3, circuit breakers of both ends are opened to clear the fault. As can be observed from the results, the proposed controller is able to well maintain the system performance even under the fault condition.

Through the studies, the effectiveness of the proposed controller against model under model uncertainty is verified.

V. Concluding Remarks

Inverter-interfaced microgrids are difficult to control due to fast dynamics, uncertainty, and a wide range of operating conditions. The virtual inertia based control solutions are simple but cannot fully unlock the potentials and advantages of such microgrids. The solutions that integrate droop-based primary control and distributed secondary control cause unnecessary V and f oscillations and cannot effectively manage the magnitude of transient line currents. To overcome these problems, control objectives should be better prioritized and power line dynamics need to be considered. The proposed control solution can not only realize better V and f control by maintaining constant $|V|$ and f references, but also ensure bounded transient line currents during normal operating conditions. By properly adjusting phase angles of bus voltages, both fair load sharing and variable uncertain operating conditions are addressed. The requirement of intersubsystem communication is also not difficult to be realized with nowadays communication techniques. The effectiveness of the proposed solution has been demonstrated through simulations.

Microgrid control is a challenging topic and deserves long-term and extensive investigation. Future work includes studying more complicated microgrid model, designing improved control algorithms, lowering communication requirements, addressing cyber uncertainties, and testing such control solutions through hardware experimentation.

References

[1] J. Rocabert, A. Luna, F. Blaabjerg, and P. Rodriguez, "Control of power converters in AC microgrids," *IEEE Trans. Power Electron.*, vol. 27, no. 11, pp. 4734–4749, Nov. 2012.

[2] Y. Li, D. M. Vilathgamuwa, and P. C. Loh, "Design, analysis and real-time testing of controller for multibus microgrid system," *IEEE Trans. Power Electron.*, vol. 19, no. 5, pp. 1195–1204, Sep. 2004.

[3] N. Pogaku, M. Prodanovic, and T. C. Green, "Modeling, analysis and testing of autonomous operation of an inverter-based microgrid," *IEEE Trans. Power Electron.*, vol. 22, no. 5, pp. 613–625, Mar. 2007.

[4] D. E. Olivares and A. M. Sani, "Trend in microgrid control," *IEEE Trans. Smart Grid*, vol. 5, no. 4, pp. 1905–1919, Jul. 2014.

[5] J. Zhao and X. Liu, "Coordinated microgrid frequency regulation based on DFIG variable coefficient using virtual inertia and primary frequency control," *IEEE Trans. Energy Convers.*, vol. 31, no. 3, pp. 833–845, Sep. 2016.

[6] H. Cai, G. Hu, F. L. Lewis, and A. Davoudi, "A distributed feedforward approach to cooperative control of AC microgrid," *IEEE Trans. Power Syst.*, vol. 31, no. 5, pp. 4057–4067, Sep. 2016.

[7] D. He, D. Shi, and R. Sharma, "Consensus-based distributed cooperative control for microgrid voltage regulation and reactive power sharing," in *Proc. IEEE PES Innov. Smart Grid Technol.*, Istanbul, Turkey, 2014, pp. 1–6.

[8] H. Xin, Y. Liu, Z. Qu, and D. Gan, "Distributed estimation and control for optimal dispatch of photovoltaic generations," *IEEE Trans. Energy Convers.*, vol. 29, no. 4, pp. 988–996, Dec. 2014.

[9] A. Maknouninejad, Z. Qu, F. Lewis, and A. Davoudi, "Optimal, nonlinear, and distributed designs of droop controls for DC microgrid," *IEEE Trans. Smart Grid*, vol. 5, no. 5, pp. 2508–2616, Sep. 2014.
[10] V. Nasirian, M. Modares, F. Lewis, and A. Davoudi, "Active loads of a microgrid as players in a differential game," in *Proc. IEEE 7th Int. Symp. Resilient Control Syst.*, 2015, pp. 1–6.
[11] L. Fan, V. Nasirian, H. Modares, F. Lewis, Y. D. Song, and A. Davoudi, "Game-theoretic control of active loads in DC microgrids," *IEEE Trans. Energy Convers.*, vol. 31, no. 3, pp. 882–895, Sep. 2016.
[12] M. Rasheduzzaman, J. A. Mueller, and J. W. Kimball, "An accurate small-signal model of inverter dominated islanded microgrids using dq reference frame," *IEEE J. Emerg. Sel. Topics Power Electron.*, vol. 2, no. 4, pp. 1070–1080, Dec. 2014.
[13] V. Nasirian, Q. Shafiee, J. M. Guerrero, and F. L. Lewis, and A. Davoudi, "Droop-free distributed control for AC microgrid," *IEEE Trans. Power Electron.*, vol. 31, no. 2, pp. 1600–1617, Feb. 2016.
[14] K. S. Narendra and S. Mukhopadhyay, "To communicate or not to communicate: A decision-theoretic approach to decentralized adaptive control," in *Proc. 2010 Amer. Control Conf. Marriott Waterfront*, Baltimore, MD, USA, 2010, pp. 6369–6376.
[15] L. Zhou, Y. Chen, A. Luo, J. M. Guerrero, and X. Zhou, "Robust two degrees-of-freedom single-current control strategy for LCL-type grid-connected DG system under grid-frequency fluctuation and grid-impedance variation," *IET Power Electron.*, vol. 9, no. 14, pp. 2682–2691, Nov. 2016.
[16] W. Guo, L. Mu, and X. Zhang, "Fault models of inverter-interfaced distributed generators within a low-voltage microgrid," *IEEE Trans. Ind. Electron.*, vol. 32, no. 1, pp. 453–461, Feb. 2017.
[17] W. Zhang, Y. Xu, W, Liu, F. Ferrese, and L. Liu, "Fully distributed coordination of multiple DFIGs in a microgrid for load sharing," *IEEE Trans. Smart Grid*, vol. 4, no. 2, pp. 806–815, Jun. 2013.
[18] W. Zhang, Y. Ma, W, Liu, S. Ranade, and Y. Luo, "Distributed optimal active power dispatch under constraints for smart grids," *IEEE Trans. Ind. Electron.*, vol. 64, no. 6, pp. 5084–5094, Jun. 2017.
[19] M. Ritwik, "Modelling, stability analysis and control of microgrid," Ph.D. dissertation, Faculty Built Environ. Eng., School Eng. Syst., Queensland Univ. Technol., Brisbane QLD, Australia, 2010, pp. 1–180.
[20] J. J. Slotine and W. Li, *Applied Nonlinear Control.* Englewood Cliffs, NJ, USA: Prentice-Hall, 1991.
[21] C. T. Chen, *Linear System Theory and Design*, 3rd ed. New York, NY, USA: Oxford Univ. Press, 1999.
[22] A. Bidram, A. Davoudi, F. L. Lewis, and J. M. Guerrero, "Distributed cooperative secondary control of microgrids using feedback linearization," *IEEE Trans. Power Systems*, vol. 28, no. 3, pp. 3462–3470, Aug. 2013.
[23] A R. Khezri, S. Shokoohi, S. Golshannavaz, and H. Bevrani, "Intelligent over-current protection scheme in inverter-based microgrids," in *Proc. Smart Grid Conf.*, Tehran, Iran, 2015, pp. 53–59.

Jiajun Duan (S'14) was born in Lanzhou, China, in 1990. He received the B.S. degree in power system and its automation from Sichuan University, Chengdu, China, and the M.S. degree in electrical engineering from Lehigh University, Bethlehem, PA, USA, in 2013 and 2015, respectively. He is currently working toward the Ph.D. degree at Lehigh University.

His research interests include power system, power electronics, control systems, renewable energy and smart microgrid.

Cheng Wang (S'12) received the B.S. degree in electrical engineering from Southwest Jiaotong University, Chengdu, China, in 2011, and is currently working toward the Ph.D. degree in electrical engineering at the School of Electrical and Electronics Engineering, Huazhong University of Science and Technology, Wuhan, China.

He is also a Research Assistant with the Department of Electrical and Computer Engineering, Lehigh University, Bethlehem, PA, USA. His research interests include microgrids, high-penetrative grid-interactive photovoltaic system, modular multilevel converters, and uninterrupted power systems.

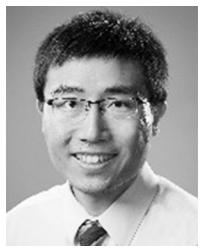

Hao Xu (M'12) was born in Nanjing, China. He received the Master's degree in electrical engineering from Southeast University, Nanjing, China, in 2009, and the Ph.D. degree in electrical engineering from Missouri University of Science and Technology, Rolla, MO, USA, in 2012.

He is currently with the University of Nevada, Reno, MO, USA, where he is an Assistant Professor with the Department of Electrical and Biomedical Engineering. His research interests include intelligent control design for advanced power systems, smart grid, autonomous unmanned aircraft systems, and wireless passive sensor network.

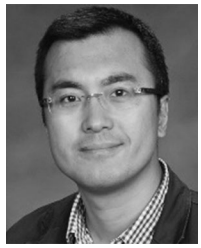

Wenxin Liu (S'01–M'05–SM'14) received the B.S. degree in industrial automation, and the M.S. degree in control theory and applications from Northeastern University, Shenyang, China, in 1996 and 2000, respectively, and the Ph.D. degree in electrical engineering from Missouri University of Science and Technology (formerly the University of Missouri–Rolla), Rolla, MO, USA, in 2005.

He is currently an Assistant Professor with the Department of Electrical and Computer Engineering, Lehigh University, Bethlehem, PA, USA. His research interests include power systems, power electronics, and controls.

Jian-Chun Peng (M'04–SM'17) received the B.S. and M.S. degrees from Chongqing University, Chongqing, China, in 1986 and 1989, respectively, and the Ph.D. degree from Hunan University, Hunan, China, in 1998, all in electrical engineering.

He is currently a Professor with Shenzhen University, Shenzhen, China, and the Director of the Department of Control Science and Engineering. He was a Visiting Professor from November 2002 to November 2003 with Arizona State University, Tempe, AZ, US, and from May 2006 to August 2006, with Brunel University, London, U.K. His research interests include smart grid optimal operation and control, power electronics application.

Hui Jiang received the B.S. degree from Chongqing University, Chongqing, China, in 1990, and the M.S. and Ph.D. degrees from Hunan University, Hunan, China, in 1999 and 2005, respectively, all in electrical engineering.

She is currently a Professor with Shenzhen University, Shenzhen, China. From November 2005 to November 2006, she was a Visiting Scholar with Brunel University, London, U.K. Her research interests include power system economics and smart grid operation.